

# Observation of Rossby waves in satellite derived chlorophyll-a data

P. Cipollini, P.G. Challenor, D. Cromwell, G.D. Quartly, and S. Raffaglio<sup>†</sup>  
Southampton Oceanography Centre, Empress Dock,  
Southampton, Hants, SO14 3ZH, UK  
email: *cipo@soc.soton.ac.uk*

<sup>†</sup>Now at Roke Manor Research, Romsey, UK

## **Abstract**

Baroclinic Rossby waves are long wavelength oceanic processes that can affect the whole of the water column. During the past decade they have been detected in sea surface height data from altimetry, with clear signals in all ocean basins. More recently they have been observed globally in datasets of sea surface temperature too. Because of their effect on the mixed layer, they may also produce an effect on the development of phytoplankton, and thus produce a signal in ocean colour data. We show westward-propagating features in chlorophyll-a data from two different spaceborne sensors and compare their characteristics with the signals in sea surface height.

## **1. Introduction**

Baroclinic Rossby waves are important oceanic processes providing a communication link between the east and west of ocean basins. These westward-propagating signals have a long wavelength (hundreds to thousands of kilometres) and a vertical structure that involves meridional movement of water in the surface layer, with reverse flow at depth. This leads to an overall change in sea surface height (SSH), which although of only a few centimetres in magnitude, can be measured by satellite altimeters. Using SSH data from TOPEX/Poseidon *Chelton and Schlax* (1996) found Rossby waves in all the main ocean basins. The latitudinal displacements of water can also lead to a change in the temperature of the surface layer. Although the skin temperature can be affected by atmospheric processes, the accurate sea surface temperature (SST) data from the ATSR instrument have shown the thermal signature of Rossby waves to be nearly ubiquitous (*Hill et al.*, 2000). *Cipollini et al.* (1997) compared the SSH and SST signals of Rossby waves in the "waveguide" at 34°N in the North Atlantic, where the eastward-flowing Azores Current appeared to increase their magnitude. Fourier analysis of the signals showed the same three baroclinic modes of propagation to be present, but with different relative strengths.

In this paper we look for the signature of Rossby waves in global ocean colour datasets, using gridded fields of chlorophyll-a from the OCTS and SeaWiFS instruments. Section 2 discusses the sources of the data and their processing; section 3 then shows various locations where clear propagating signals can be seen. The Radon transform is used in section 4 to show that the dominant propagating signals are consistent with those expected for Rossby waves. In section 5 we provide a brief summary, along with a discussion of the interpretation of these results.

## 2. Ocean colour datasets

### 2.1 OCTS

The ADEOS satellite, launched in August 1996, contained a number of instruments designed for Earth observation, amongst them the Ocean Color and Temperature Scanner (OCTS). This collected data in 12 channels, spanning 412 nm to 12  $\mu\text{m}$  (see Fig. 1), with the chlorophyll-a content being determined from a combination of channels in the visible region of the spectrum, after a correction has been applied for varying atmospheric aerosol content using information from the near infra-red channels. The data we use here are version 4 of the monthly product provided by NASDA-EORC. Unfortunately the extent of the data is only 8 months due to the early demise of the satellite.

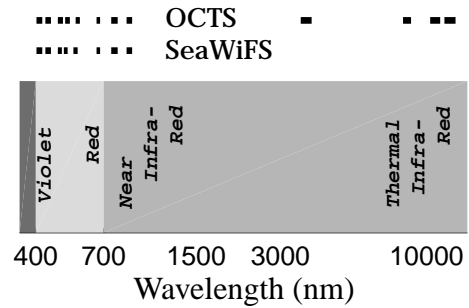


Fig. 1: Location of OCTS and SeaWiFS channels within the electromagnetic spectrum.

### 2.2 SeaWiFS

The OrbView-2 satellite, launched in August 1997, is dedicated to observing ocean colour, with its Sea-viewing Wide Field-of-view Sensor (SeaWiFS) operating in 8 channels spanning 412 nm to 865 nm (see Fig. 1). We use here version 3 of the chlorophyll-a product provided by NASA/GSFC DAAC.

### 2.3 Initial Processing

Both the OCTS and SeaWiFS monthly composites are provided on a  $0.0879^\circ \times 0.0879^\circ$  grid. We rebin the data on to a  $0.5^\circ \times 0.5^\circ$  grid, using a Gaussian interpolator with a half-width of 150km. This is done because we are only interested in large scale coherent features. Any gaps remaining due to persistent cloud cover are filled by Kalman filtering. In many regions the resultant dataset shows a very strong seasonal signal associated with a bloom of the phytoplankton, as can be seen in the Hovmöller diagram for  $34^\circ\text{S}$  (see Fig. 2). Peak chlorophyll values occur during the austral spring bloom. Note the use of a logarithmic colour scale to bring out the subtle variations at low chlorophyll contents.

To suppress the seasonal variation we apply a high-pass filter in the zonal direction. As a change in chlorophyll concentration is likely to be proportional to the quantity already present, we

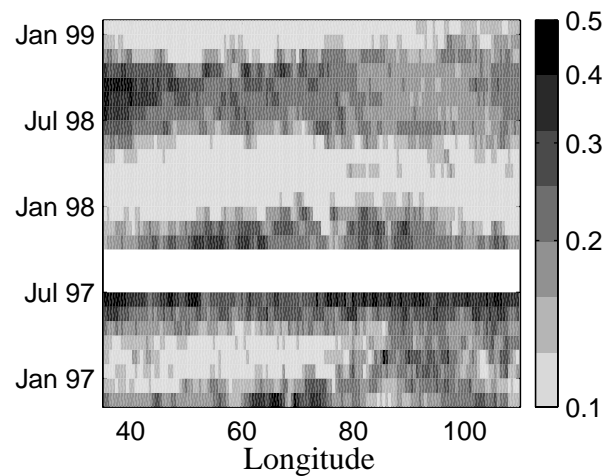


Fig. 2: Hovmöller diagram of chlorophyll-a content data (in  $\text{mg m}^{-3}$ ) at  $34^\circ\text{S}$  in the Indian Ocean. [The first 8 months data are from OCTS; the rest, after a 3-month gap, are from SeaWiFS.]

take the logarithm of the dataset before applying the high-pass filter to give fractional changes (see Fig. 3a).

### 3. Discussion of Hovmöller diagrams

We applied the processing detailed above to all latitudes in the Indian Ocean from 38°S to 10°N. Diagonal alignments of fractional changes were readily apparent at all latitudes between 35°S and 11°S (see Fig. 3 for examples); further north there were no clear signals, with gaps in the data due to land or else anomalously high chlorophyll content fixed in one location, presumably associated with an upwelling regime that did not change. We discuss below the three examples shown in Fig. 3.

At 34°S (Fig. 3a) individual features can be traced throughout the coverage by SeaWiFS, moving west by about 12° in the 16 months of data shown; however the clarity of the signal varies seasonally, being most apparent around January, when the phytoplankton bloom is just dying off (cf. Fig. 2). It is also quite clear in June, at the onset of the bloom. Similar features can be seen in the short extent of OCTS data.

At 26°S (Fig. 3b) there are again some coherent features propagating westward, but they are not as pronounced, despite the contrast being enhanced to a greater extent than for Fig. 3a. With care it can be seen that the propagation rate here is faster, and there is also an eastward-propagating signal, which passes through 70°E in June 1997 at the end of the OCTS dataset, and can then be followed in the SeaWiFS data too. The fixed feature at 45°E coincides with the waters just to the south of Madagascar, and it is conjectured that there may be consistently high phytoplankton growth there due to upwelling of nutrients.

At 13°S (Fig. 3c) there are again strong propagating signals in the ocean colour data, with a much faster speed than in the other two locations shown. There is a small data gap at ~48° E associated with the northern tip of

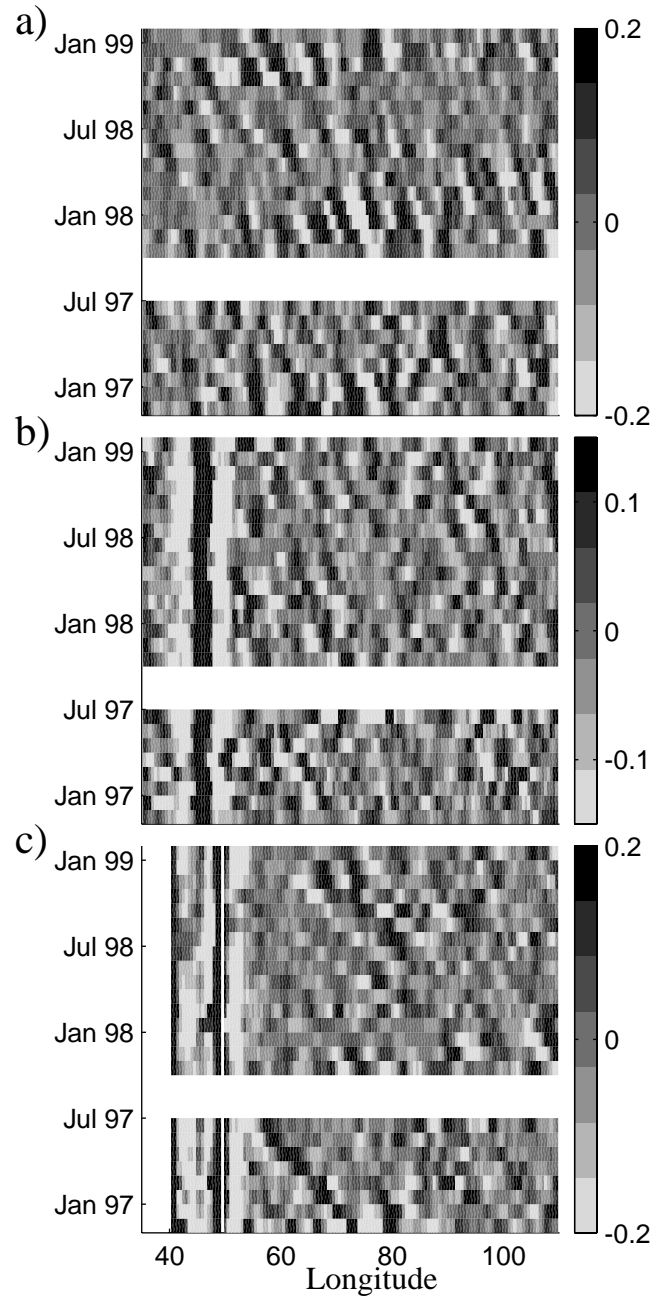


Fig. 3: Filtered Hovmöller diagrams of chlorophyll-a content at three locations in the Indian Ocean. a) 34°S, b) 26°S, c) 13°S. [Natural logarithms were taken, before applying a high-pass filter to give anomalies relative to local mean; thus '0.1' represents a change of  $e^{0.1}$  i.e. 10.5%.]

Madagascar. The seasonal modulation is not as strong as at 34°S.

The features shown in Fig. 3 appear consistent with Rossby waves; they head westward, have wavelengths of several degrees (hundreds of kilometres) and are faster the nearer they are to the equator. As the speed of Rossby waves has been a keen research topic of late for both theoreticians and observers, we concentrate here on an accurate objective method of determining their speed.

#### 4. Application of Radon Transform

One technique that is specifically designed for detecting lines in an image is the Radon transform (Deans, 1983). We use this to find how much power is associated with each speed (direction in the Hovmöller plot). For this we constrain our data to the range 65°E to 104°E and for all latitudes 35°S to 11°S. This restricted domain avoids any permanent local anomalies, such as associated with particular upwelling regions. We also only analyse the period of SeaWiFS data to overcome the problem of missing data. We follow the approach used by Cipollini *et al.* (1999) with SSH data in the northeast Atlantic, and record the power of the signal perceived by the Radon transform for all speeds, rather than just selecting the speed with the strongest signal at each latitude.

Figure 4a shows the results, which indicate that all latitudes between 35°S and 11°S have a dominant signal heading west and that the speeds are greater nearer the equator. The signal is more pronounced in the band 35°S to 31°S and 17°S to 11°S than at the latitudes inbetween. This does not mean that the Rossby waves are weaker between 30°S and 18°S, but just that their manifestation in the ocean colour dataset is not as strong. Also for many latitudes north of 17°S there is evidence of two distinct propagation speeds, with the weaker one half the speed of the stronger. These may possibly be different Rossby modes (as discussed in the northeast Atlantic by Cipollini *et al.* (1997) and in the Indian Ocean by Subrahmanyam *et al.* (2000).

For comparison, a similar Radon Transform analysis was carried out for SSH data derived from the TOPEX/Poseidon satellite (Fig. 4b). Similar results are noted, with an even clearer absence of consistent eastward-propagating features. There is a good agreement in the dominant speeds for latitudes south of 20°S, but in the tropical region the SSH signals are notably faster than those in ocean colour. It is also interesting that in the altimetry, the latitude range 28°S to 20°S is one of strong Rossby signals.

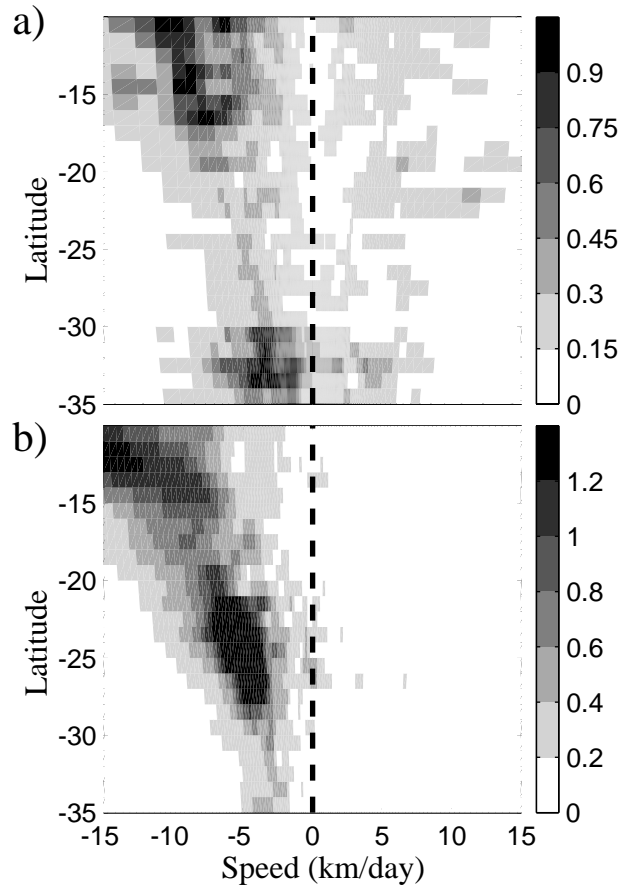


Fig. 4: Intensity of power from Radon transform associated with different propagation speeds for latitudes between 35°S and 11°S inclusive. Negative speeds imply westward propagation, and units for the 2 plots are arbitrary and different. a) SeaWiFS data, b) TOPEX/Poseidon data.

## **5. Summary and Discussion**

Many authors have shown evidence for oceanic Rossby waves using sea surface height and temperature data. Here we have shown that, for a large part of the Indian Ocean, there is compelling proof that they can be detected in the surface concentrations of phytoplankton. Whilst Machu *et al.* (1999) had earlier found wave-like signals in SeaWiFS data in the southwest Indian Ocean, they were only showing a spatial periodicity in the meanders of the Agulhas Return Current about a latitude of 38°S, rather than demonstrating propagating signals. Our analysis has separately examined a range of latitudes (35°S to 11°S), all to the north of the subtropical convergence, and found westward propagating features within both the OCTS and SeaWiFS datasets. An examination of phase speed revealed propagation rates *similar* to those observed by altimetry; however questions remain as to whether the ocean colour signal may sometimes represent a higher order mode of Rossby waves.

There are two distinct mechanisms by which a Rossby wave can affect the concentration of phytoplankton in surface waters. The first is purely physical — the lifting of more biota into the observing depth as the thermocline is raised. The alternative is biological and longer-lasting — a growth in the quantity of phytoplankton in response to increased upwelling of nutrients. [We are sure that the Rossby waves signals that we see in ocean colour are not a result of SST variations through into the atmospheric corrections, as the chlorophyll algorithms for both sensors make no use of thermal infra-red channels, and there are no similar propagating features in other derived products such as aerosol thickness.]

At present there is only a small temporal overlap between the data we have from the SeaWiFS and TOPEX/Poseidon instruments. However in the future we hope to correlate anomalies in the SSH and ocean colour fields, as their relative phase may help clarify the mechanisms responsible for the ocean colour signature of Rossby waves.

### **Acknowledgements**

We thank NASDA/EORC for the OCTS data, NASA/GSFC DAAC for the SeaWiFS data and AVISO/Altimetry for the TOPEX/Poseidon data. We are grateful to Helen Snaith for help in the processing of the altimetry data, and to Meric Srokosz for many animated discussions.

### **References**

- Chelton, D.B. and M.G. Schlax, 1996, Global observations of oceanic Rossby waves, *Science*, **272**, 234-238.
- Cipollini, P., D. Cromwell, M.S. Jones, G.D. Quartly and P.G. Challenor, 1997, Concurrent altimeter and infrared observations of Rossby wave propagation near 34°N in the northeast Atlantic, *Geophys. Res. Lett.*, **24**, 889-892.
- Cipollini, P., D. Cromwell and G.D. Quartly, 1999, Observations of Rossby wave propagation in the northeast Atlantic with TOPEX/POSEIDON altimetry, *Adv. in Space Res.*, **22**, 1553-1556.
- Deans, S.R., 1983, The Radon transform and some of its applications, published by John Wiley, New York]
- Hill, K.L., I.S. Robinson and P. Cipollini, 2000, Propagation characteristics of extratropical planetary waves observed in the global ATSR sea surface temperature record, *J. Geophys. Res.* (in press).
- Machu, E., B. Ferret and V. Garçon, 1999, Phytoplankton pigment distribution from SeaWiFS data in the subtropical convergence zone south of Africa: A wavelet analysis, *Geophys. Res. Lett.*, **26**, 1469-1472.
- Subrahmanyam, B. I.S. Robinson, J.R. Blundell and P.G. Challenor, 2000, Rossby waves in the Indian Ocean from TOPEX/POSEIDON altimeter and model simulations, *Int. J. Rem. Sensg.* (in press).